Development of induced glioblastoma by implantation of a human xenograft in Yucatan minipig as a large animal model

Mehrdad Khoshnevis, Claude Carozzo, Catherine Bonnefont-Rebeix, Sara Belluco, Olivia Leveneur, Thomas Chuzel, Elodie Pillet-Michelland, Matthieu Dreyfus, Thierry Roger, François Berger, et al.

Journal of Neuroscience Methods 282 (2017) 61–68

Contents lists available at ScienceDirect

Journal of Neuroscience Methods

journal homepage: www.elsevier.com/locate/jneumeth

Research Article

Development of induced glioblastoma by implantation of a human xenograft in Yucatan minipig as a large animal model

Mehrdad Khoshnevis[a,*], Claude Carozzo[a], Catherine Bonnefont-Rebeix[a], Sara Belluco[a], Olivia Leveneur[c], Thomas Chuzel[d], Elodie Pillet-Michelland[a], Matthieu Dreyfus[e], Thierry Roger[a], François Berger[e], Frédérique Ponce[a,b]

[a] ICE (Interactions Cellules Environnement), UPSP 2016.A104, VetAgro Sup, Campus Vétérinaire de Lyon,1 avenue Bourgelat, 69280, Marcy l'Etoile, France
[b] Clinical Oncology Unit, VetAgro Sup, Campus Vétérinaire de Lyon,1 avenue Bourgelat, 69280, Marcy l'Etoile, France
[c] BIOVIVO, Institut Claude Bourgelat, VetAgro Sup, Campus Vétérinaire de Lyon,1 avenue Bourgelat, 69280, Marcy l'Etoile, France
[d] Voxcan,1 avenue Bourgelat, 69280 Marcy l'Etoile, France
[e] Grenoble Alpes University, Inserm Unit 1205, 17 rue des Martyrs-Bât. 4023, 38054 Grenoble, France

HIGHLIGHTS

- We developed the U87 glioblastoma model in Yucatan minipig.
- The period of development was short approximately 28 days.
- Minimum blood level of cyclosporine is important to develop GB in Yucatan.
- Brain similarities of minipig and human make it a good model for preclinical studies.
- Yucatan is an affordable animal model regarding the low cyclosporine and caring cost.

ARTICLE INFO

Article history:
Received 9 February 2017
Accepted 7 March 2017
Available online 9 March 2017

Keywords:
Minipig
Yucatan
Glioblastoma
U87
Cyclosporine
Animal model

ABSTRACT

Background: Glioblastoma is the most common and deadliest primary brain tumor for humans. Despite many efforts toward the improvement of therapeutic methods, prognosis is poor and the disease remains incurable with a median survival of 12–14.5 months after an optimal treatment. To develop novel treatment modalities for this fatal disease, new devices must be tested on an ideal animal model before performing clinical trials in humans.
New method: A new model of induced glioblastoma in Yucatan minipigs was developed. Nine immunosuppressed minipigs were implanted with the U87 human glioblastoma cell line in both the left and right hemispheres. Computed tomography (CT) acquisitions were performed once a week to monitor tumor growth.
Results: Among the 9 implanted animals, 8 minipigs showed significant macroscopic tumors on CT acquisitions. Histological examination of the brain after euthanasia confirmed the CT imaging findings with the presence of an undifferentiated glioma.
Comparison with existing method: Yucatan minipig, given its brain size and anatomy (gyrencephalic structure) which are comparable to humans, provides a reliable brain tumor model for preclinical studies of different therapeutic
Methods: in realistic conditions. Moreover, the short development time, the lower cyclosporine and caring cost and the compatibility with the size of commercialized stereotactic frames make it an affordable and practical animal model, especially in comparison with large breed pigs.
Conclusion: This reproducible glioma model could simulate human anatomical conditions in preclinical studies and facilitate the improvement of novel therapeutic devices, designed at the human scale from the outset.

1. Introduction

Glioblastoma (GB) is the most common and aggressive primary malignant brain tumor in adults (Dréan et al., 2016; Louis et al., 2016) for which no certain cure is available (Burger et al., 1985;

* Corresponding author.
E-mail addresses: mehrdad.khosh-nevis@vetagro-sup.fr, dvm.khoshnevis@gmail.com (M. Khoshnevis).

http://dx.doi.org/10.1016/j.jneumeth.2017.03.007
0165-0270/

Ferreira et al., 2016). GB leads to death in most patients because of the highly invasive character and infiltration into brain parenchyma (Mujokoro et al., 2016). It is typically confined to the central nervous system (CNS) and does not metastasize outside (Omuro and DeAngelis, 2013). GB accounts for almost 25% of all primary CNS tumors and 55% of all the gliomas with an annual incidence of 3.2 per 100,000 (Allahdini et al., 2010; Thakkar et al., 2014). GB has the highest number of cases among all malignant tumors with an incidence estimation of 12,120 new cases in 2016 (Ostrom et al., 2016). After the first treatment, the majority of all GB patients experience disease progression (Omuro and DeAngelis, 2013). The prognosis of GB is very poor and long-term survivals are rare.

GB management remains palliative and includes the standard treatments of brain tumors, being surgery, radiotherapy and chemotherapy. Cancer immunotherapy is under investigation as an additional treatment modality (Weiss et al., 2016). Today, postoperative radiotherapy combined with concurrent and adjuvant temozolomide (TMZ) as a systemic chemotherapy is the standard treatment method (Hingorani et al., 2012; Johnson and O'Neill, 2012; Omuro and DeAngelis, 2013; Stupp et al., 2005; Walid, 2008). Unfortunately, after an aggressive total surgical resection, GB still remains non-curative because of the infiltrative property of the tumor (Tate and Aghi, 2009; Zagzag et al., 2000). It progresses diffusely and commonly recurs locally within 2 cm of the original tumor bed (Ashby et al., 2016). The therapeutic potential of radiotherapy alone is limited due to the inherent radio-resistance of GB cells (Shaifer et al., 2010). Brachytherapy and stereotactic radiosurgery are used for relapsed GB but tend to be associated with notable toxicity (Barani and Larson, 2015). In addition, the blood brain barrier (BBB) is a major limitation, reducing efficacy of anti-cancer drugs in the treatment of GB patients. The passage of anti-tumor agents through the BBB is poorly and heterogeneously documented in the references (Dréan et al., 2016). Despite all efforts to improve the treatment methods, the overall outcome remains poor. With an optimal treatment, the disease remains incurable with a median survival of approximately 12 and 14.5 months after adjuvant radiation and temozolomide-based chemoradiotherapy, respectively (Hingorani et al., 2012; Yang et al., 2015). Beyond this period, the survival rates 2 and 3 years after diagnosis are 26.5% and 2%, respectively (Thomas et al., 2012; Walid, 2008).

These limitations make it essential to administrate high drug concentrations for treatment, potentially exposing patients to severe toxicity and side effects. Therefore, to circumvent the BBB and other restricting factors, novel therapeutic approaches, such as the injection of therapeutic agents directly into the tumor, are advocated to prolong survival time (Cokgor et al., 2000; Kikuchi et al., 2002; Lidar et al., 2004). For this kind of treatment modality, the main issues are the reflux and the leakage after the injection (Buonerba et al., 2011). Reflux is when the fluid flows towards the outside of the tumor through the injection canal. It causes an injected distribution in the tumor that differs from that which was planned. This phenomenon is mainly due to the tumor density. It normally happens if the injection rate exceeds the diffusion rate within the tumor. The second pitfall is the leakage of therapeutic agents during intracerebral injection, which is usually due to the brain ventricles and the cortical sulci near to the injection location (Acabchuk et al., 2015; Selek et al., 2014).

The rodent brain is lissencephalic, meaning that the outer cerebral cortex is smooth and the brain does not contain the sulci (Howells et al., 2010; Semple et al., 2013). This anatomical property, minimizes leakage and improves local drug delivery during infusion in animal experiments (Sampson et al., 2007). Murine animal models, both xenograft and genetically engineered, are most commonly used for cancer research due to the relatively fast generation time (Chen et al., 2013; McNeill et al., 2015; Oh et al., 2014). However their brain lacks the development of the cortex in comparison to primates or larger animals (Sauleau et al., 2009; Semple et al., 2013). The complexity of the human tumor microenvironment and the difference between the brain anatomy of humans and rodents could explain why the majority of successful cancer therapies administered in small animal models cannot be reproduced with humans. This results in a failure in clinical studies and fails to obtain similar efficacy in patients (Buonerba et al., 2011; Chen et al., 2013). Developing a cerebral tumor in a large animal model would be very useful in preclinical studies to assess and investigate intratumoral injections in relatively similar conditions to humans. A spontaneous dog glioma model (brachycephalic breeds) exists, but this tumor is quite rare in dogs and constitutes a non-reproducible model (Chen et al., 2013; Dickinson et al., 2010). Among the different large animal species, pigs are an ideal model in settings requiring human-like brain anatomy, histology and vascularization (Lind et al., 2007; Sauleau et al., 2009; Schook et al., 2015). The gyrencephalic structure of the pig brain is more similar to human in terms of development compared to the lissencephalic (smooth) brain of common small laboratory animals (Lind et al., 2007). Furthermore, the use of pigs is less expensive and poses fewer ethical concerns than the use of non-human primates, especially when accurate behavioral measurements are not necessary (White et al., 2011). The major benefit of the porcine model for neuroscience research is its brain size. These advantages cause this model to be obviously superior to rodent for preclinical testing and also make it compatible with high-resolution imaging platform used in clinical trials (Sauleau et al., 2009; Snyder et al., 2006). However, the high body weight of mature pigs of large breeds, which can be as much as 2,50,300 kg, presents an obvious disadvantage. This restriction sets the upper age limit of research pigs at only the first few months after birth. Therefore, in terms of weight, a reasonable alternative to large breed pigs would be the minipigs. An immunosuppressed strain is essential if human cell lines are inoculated as xenografts to generate the tumors and to avoid the rejection of injected cells (Michel-Monigadon et al., 2010). In this study, a minipig model with a human brain tumor is developed by implantation of human GB cell line (U87) in both left and right hemispheres with different cell concentrations to assess the tumor growth and evaluate the imaging and pathological findings. Cells were implanted bilaterally to increase tumor take rate in each animal and consequently to decrease for ethical concerns the number of enrolled animals for subsequent research purposes.

2. Materials and methods

2.1. Animals

Yucatan minipigs were selected for the GB development study. Nine animals between 3–4 months old, both male and female, were purchased from INRA Saint-Gilles, France. They were transferred to the Claude Bourgelat institute in Marcy l'Etoile, France to be kept 7–10 days for acclimatization before surgery. The minipigs were regularly examined by a veterinarian to check for any congenital or infectious diseases before administration of the immunosuppressive treatment. The presence of any disease was a criterion for removing the animal from the study. Minipigs were kept at a temperature of 19 °C, with humidity >35% and ventilation at least 10 times/hour. The feed was provided by the breeder, with an intake of 350–400 g/day/animal.

2.2. Ethical considerations

The experimental protocol was reviewed and approved by the VetAgro Sup Ethical Committee (1522_V2) and received official authorization by the French Ministry of Scientific Research

(2015052012034148_v1). All aspects of care and the use of the animals, including surgical procedures and pain assessment, were performed and monitored in compliance with French regulations (transposition of Directive 2010/63/EU) and the local Animal Welfare Body.

2.3. U87 cells preparation

U87 cells were chosen because they were used in a previous study on large landrace pigs (Selek et al., 2014). Cells were obtained from the American Type Culture Collection (Manassas, VA, USA). For inoculation of U87 cells in each subject, U87 cells were plated in 2 T175 tissue culture flasks with a density of 0.8–1.2 $\times$ 10^6 cells per flask. Cells were grown in Minimum Essential Media (MEM) medium supplemented with 10% fetal calf serum, 100 U/ml penicillin, 100 μg/ml streptomycin, 2 mM L-Glutamine and 0.25% g/mL amphotericin B. Cells were maintained at 37 °C in a humidified CO_2 (5%) atmosphere, and the medium was changed every 3 days. A week later, cells from these flasks were trypsinized with 0.25% trypsin-EDTA and then 35–50 $\times$ 10^6 cells per flask were harvested. Cells were washed twice in PBS before being pelleted 4 min at 3000 g in a 2 ml Eppendorf vial just before the inoculations. The final cell concentration in each Eppendorf vial was about 1.7 $\times$ 10^6cells/10 μl. For each subject, 40 μl and 20 μl of the cells pellet were drawn up into the syringe and injected into the right and left hemisphere, respectively.

2.4. Stereotactic system

A large animal stereotactic frame (RWD, 68901) was used to perform intracerebral stereotactic injections of tumor cells. Using different adaptors, the frame is applicable to most of large laboratory animals. Using a stereotactic frame had the advantage of being able to perform the injections as accurately as possible according to the coordinates of injection location obtained by the pre-operative CT-Scan.

2.5. Surgical procedure

The minipigs were pre-medicated with an intramuscular injection of azaperone (Stresnil®) and atropine sulfate. After 15–20 min, the anesthesia was induced by intramuscular injection of Tiletamine + Zolazepam (Zoletil® 100). An isotonic solution was continuously administered through a catheter. Under orotracheal intubation, the sedation was maintained by inhalation of isoflurane 2% in Oxygen. The animals were given the analgesic: morphine hydrochloride (Aguettant®) and antibiotic treatments: Amoxicillin + Clavulanic acid (Augmentin®) before starting the surgery. During the operation, the functionality of the cardio-respiratory system was monitored. In the case of showing any sign of pain, morphine was administered throughout the intervention. For the cell injection, each animal was positioned on the operating table, fixing the head in the stereotactic frame. The tooth bar and ear bars were inserted into the mouth and ear canal, respectively, to reach the optimal positioning and the maximum immobilization of the head during the surgery. Before draping, the surgical location was disinfected with povidone-iodine (Vetedine savon®) and sterile water. The skull skin was cut with a 4–5 cm longitudinal incision along the midline, anterior to the occipital crest. The periosteum was medially incised and elevated to clear the skull bone and its suture lines. According to the brain coordinates obtained by the pre-operative CT images, the skull was drilled usually at 30 mm anterior to the occipital crest and 7 mm to the right and left of midline without crossing the dura-mater. The thickness of the skull bone was normally less than 3 mm in this location. Size of the holes was approximately 4–5 mm in diameter. U87 cells were slowly injected through the openings in the left (3.5 $\times$ 10^6cells/20 μl) and right (7 $\times$ 10^6 cells/40 μl) hemispheres. The injection area was in the corpus striatum usually in 9–10.5 mm of depth, between the dura-mater and the brain ventricle. The stereotactic cell injections were performed with a 50 μl Hamilton syringe with a 25 gauge needle with the aid of a syringe pusher to ensure an injection rate of 20 μl/min. To prevent the reflux of injected cells, a 1 min pause was imposed before gradually withdrawing the needle from the brain. The holes were closed with fatty tissue to prevent the formation of adherences or scar tissues in the holes during the period of tumor growth. Periostum was sutured and skin incision was closed in two separate layers. After extubation, the animal was transferred to the recovery room for post-operative monitoring. A pain reliever was supplied via a Fentanyl patch 25 μg/h. Morphine was administered every 4 h until patch efficiency wore off. Prophylactic antibiotic (Kesium) was administered until 6 days after the surgery. To prevent the cerebral edema, corticotherapy (Dexamethasone) was carried-out for the 3 days following the implant.

2.6. Immunosuppression

As described, the human glioblastoma U87 cell line was implanted into Yucatan minipigs. To avoid rejection of the grafted cells, cyclosporine (Neoral® 100 mg/ml) was administered (25 mg/kg) twice a day. The goal was to maintain the blood level of cyclosporine above 1000 μg/L. Several blood samples were taken to observe the cyclosporine level in the serum. The administration continued until animal euthanasia.

2.7. CT-Scan imaging

CT acquisitions were realized at Voxcan (Marcy l'Etoile, France) with an anatomical imaging system (GE BrightSpeed 16). A standard protocol of acquisition was selected using the parameters: Tension: at 120 kV and Amperage at 150 mA. Imaging was done with a pixel size of 391 μm and a slice thickness of 625 μm describing a field of view (FOV) of 25 cm diameter centered on the pig's head. During the CT acquisition, the minipig was positioned at ventral decubitus and was under general anesthesia with the same protocol as for the surgery. On the day of implantation, before starting the intervention, a pre-operative acquisition was first performed to assess the skull thickness and to verify the absence of any abnormalities or congenital complications in the brain. Tumor progression was evaluated with CT acquisitions on days 7, 14, 21, 28 post-implantation. Tumor segmentations were done after each CT acquisition to determine the tumor volume (cm^3).

2.8. Euthanasia

Once a 1 cm tumor was observed in CT images, daily examination of minipigs was started to assess their neurological condition and to find any clinical sign related to the brain tumor. Animals who presented untreatable neurological symptoms, such as ataxia, complete epilepsy and recumbency, were anesthetized with Zoletil® as described above and sacrificed by intracardiac administration of pentobarbital (Dolethal®) 200 mg/ml, resulting in an immediate and painless death. The brain was quickly removed and fixed in a 4% formalin solution for histological examination.

2.9. Histopathology

Histological examination was carried out to confirm the CT imaging findings. Fixed samples were processed and embedded in paraffin. For each tumor, a 4 μm section was stained with hematoxylin and eosin. In one case, four additional sections were

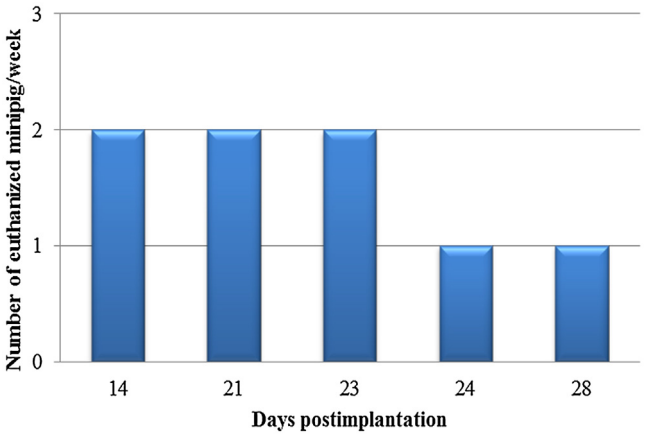

Fig. 1. Number of sacrificed minipigs with GB per week, after U87 cells implantation (n = 8). The minipig with regressed tumor is not considered in this figure.

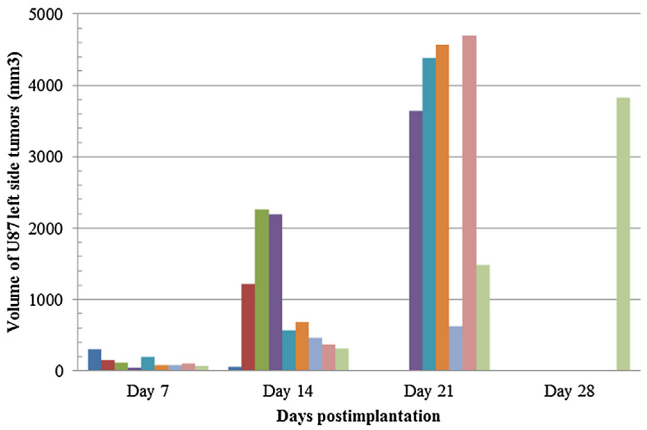

Fig. 3. Volume of U87 tumors induced in left hemispheres. The volumes based on CT Images 7, 14, 21 and 28 days after implantation. The number of injected cells in this hemisphere: (3.5×10^6cells/20 μl). Each histogram bar corresponds to a minipig. Two minipigs were euthanized before CT acquisition at day 21 and seven ones before day 28. The minipig with regressed tumor is not considered after day 14.

obtained to be used for immunohistochemistry. Immunohistochemical stains were performed with the avidin-biotin-peroxidase complex method, using the following antibodies specific for: glial fibrillary acid protein (GFAP, diluted 1:200, Dako, Carpinteria, California, United States), S-100 (S-100B, diluted 1:400, Dako), and vimentin (clone V9, diluted 1:50, Dako). For all the applied antibodies, except for GFAP, antigen retrieval was performed by heating at 90 °C for 40 min in citrate tampon, followed by a 20 min cool off. A negative control was performed by omitting the primary antibody.

3. Results

3.1. Tumor development

Nine minipigs were implanted with the U87 cells. Among them, eight minipigs presented the GB in the subsequent CT images. Continuous tumor growth led to neurological symptoms (ataxia, complete lateral recumbency) within the follow-up period 14–28 days after tumor implantation. The number of euthanized minipigs per week is presented in Fig. 1: two were euthanized at day 14, two at day 21, two at day 23, one at day 24 and one at day 28 post-implantation. In one minipig, both side tumors developed well within the first 14 days post-implantation, but tumors regression was observed after this time. The regression occurred once the whole-blood concentration of cyclosporine was lower than 1000 μg/L. This minipig was sacrificed at day 28 after the last CT acquisition. Its data after day 14 post-implantation are not considered in the figures and table.

3.2. CT-Scan images

Post-implant CT acquisitions were performed once a week (days 7, 14, 21, 28) until observing severe clinical symptoms in each ani-

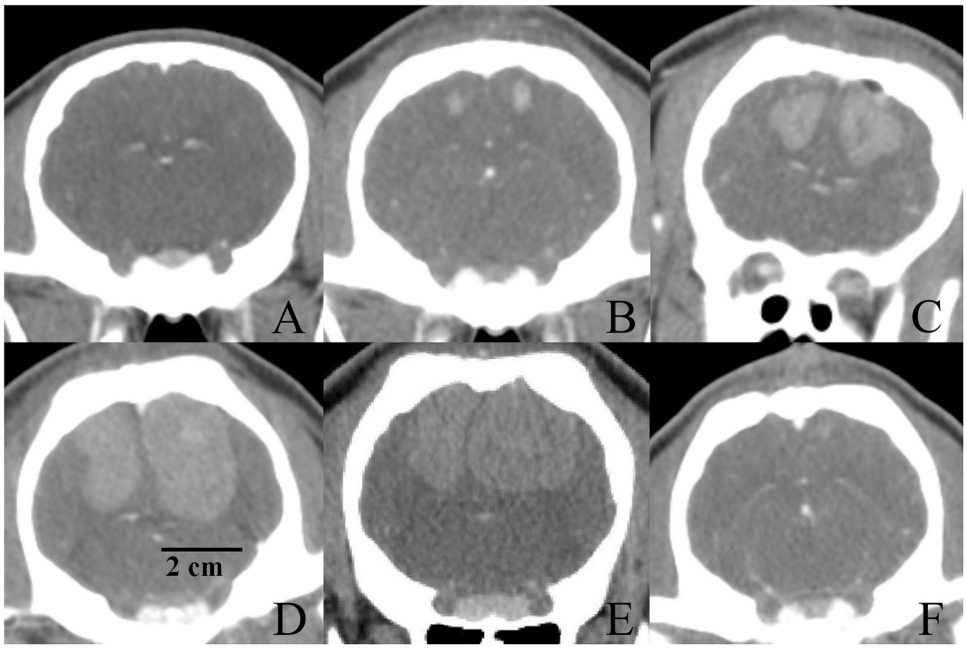

Fig. 2. Representative example of the U87 GB images in Yucatan minipigs. The number of injected cells in right and left hemispheres are (7×10^6cells/40 μl) and (3.5×10^6cells/20 μl), respectively. (A) Injection area before cells implantation at day 0, (B) Tumor size approximately 3 mm in right side tumor 7 days after implantation, (C) tumor of euthanized minipig at day 14 post-implantation, (D) tumor of euthanized minipig at day 21 post-implantation, (E) tumor of euthanized minipig at day 28 post-implantation, (F) tumor regression in one minipig, imaging at day 28 post-implantation, before euthanasia.

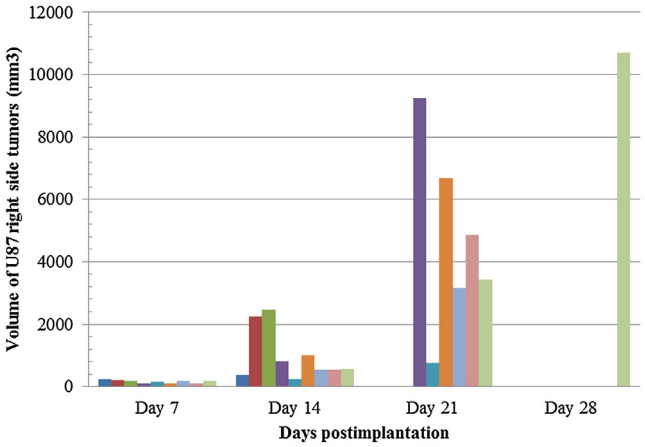

Fig. 4. Volume of U87 tumors induced in right hemispheres. The volumes based on CT Images 7, 14, 21 and 28 days after implantation. The number of injected cells in this hemisphere: (7×10^6cells/40 μl). Each histogram bar corresponds to a minipig. Two minipigs were euthanized before CT acquisition at day 21 and seven ones before day 28. The minipig with regressed tumor is not considered after day 14.

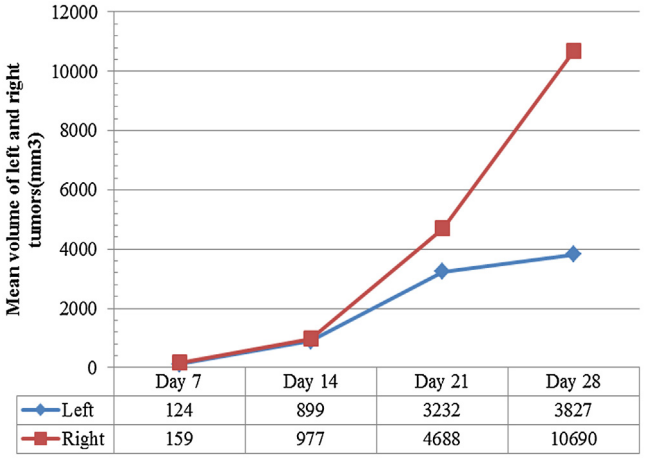

	Day 7	Day 14	Day 21	Day 28
Left	124	899	3232	3827
Right	159	977	4688	10690

Fig. 5. Mean volume of tumors implanted in the left and right hemispheres. The volumes based on CT Images 7, 14, 21 and 28 days after implantation. The number of injected cells in left and right hemispheres are (3.5×10^6cells/20 μl) and (7×10^6cells/40 μl), respectively. The minipig with regressed tumor is not considered after day 14.

mal. All the tumors displayed a slight increase in density compared with adjacent cerebral parenchyma, with clear boundaries and a plurilobed form. After injection of contrast product, there was a significant and homogeneous marking of the tumor with lack of mineralization foci. There was no evidence of hemorrhage after cell implantation. (Fig. 2)

Tumor volumes were determined by a manual segmentation of each tumor using the acquired CT Images 7, 14, 21 and 28 days following the implantation (Table 1, Figs. 3, 4). The mean volumes of the U87 tumors in the left and right hemispheres are presented in Fig. 5.

3.3. Anatomopathological findings

In the samples of 8 minipigs, an undifferentiated tumor, consistent with GB, was present. Macroscopically, the implanted tumors were gray to red in color and distinguishable from surrounding tissue in terms of texture. The size of tumors at the moment of brain sampling after euthanasia was between 1.5 and 3 cm (Fig. 6). Histologically, the tumors were mainly located within the gray and white matter of the parietal lobes. They were well delimited, not

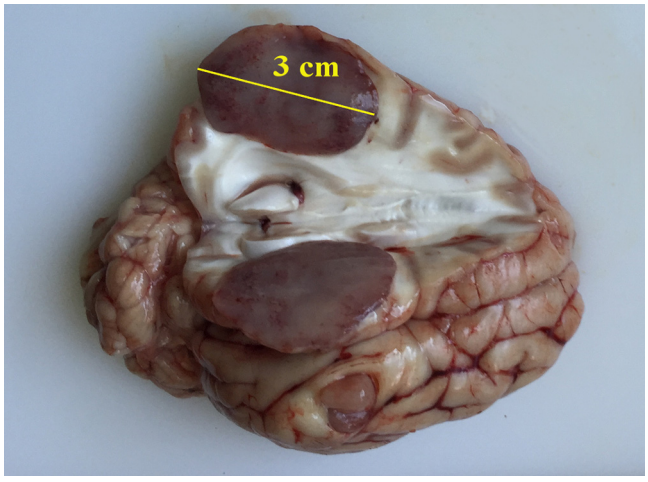

Fig. 6. Macroscopic image of the U87 induced tumor in sagittal section. An oval 3 mm mass is present in the left hemisphere (parietal lobes), replacing the gray matter and extending into the white one. It is firm, well delimited gray to red in color because of some intra-tumoral hemorrhages. (For interpretation of the references to colour in this figure legend, the reader is referred to the web version of this article.)

encapsulated and highly cellular. They were composed of sheets and bundles of polygonal to spindle cells in a scant fibrovascular stroma. The nucleo-cytoplasmic ratio was moderate. The cytoplasm was eosinophilic and the nuclei were round to irregular, centrally located, with a mottled chromatin and contained 1 or 2 nucleoli. Anisocytosis and anisokaryosis were moderate to severe. Mitoses were up to 10 per high-power field (400×). Tumoral cells presented a pseudopalisadic arrangement around the necrotic foci. In some samples, a moderate number of lymphocytes were present around the tumor (Fig. 7). Tumoral cells were strongly positive for vimentin but negative for GFAP and S-100 (Fig. 8). In the minipig in which the tumor regression started after day 14, no visible macroscopic lesions were present after euthanasia at day 28. Also, no histological lesions were observed on the slides.

4. Discussion

In this study, a GB model was developed by implanting the U87 cell line in Yucatan minipigs as a large animal model of human brain tumor. The U87 GB model is a common model for the development of GB and is a highly malignant glioma clone that comes from a 44 year-old cancer patient (Pontén, 1975; Strojnik et al., 2010). This human cell line was selected because of its highly invasive property and its rapid proliferation rate both in mice and pigs (Selek et al., 2014). Researches have shown that the prosperity of tumor development in animal models diminishes with lower histological grades (Krementz and Greene, 1953) and good transplantability is correlated to the tumor malignancy (Greene, 1952; Huszthy et al., 2012). Another attractive characteristic was the radioresistance of the U87 cell line. Due to this fact, positive outcomes of novel radiotherapy methods on this GB model could be strongly reliable and reproducible in clinical studies in humans. Today, several GB models in small and large animals exist, but clearly, none of the developed animal models can perfectly represent human GB development and progression. For example, the murine model for primary brain tumors has developed over the last 60 years, and notable improvements have been achieved with the validation of invasive GB models (Huszthy et al., 2012), but when the results of therapeutic trials were evaluated in humans, they failed in phase 2 or 3 of clinical studies. According to different studies, glioma cell lines grown in rodent animal models were unreliable in predicting clinical results for a translational purpose (Dinapoli et al., 1993;

Table 1
Left and right side tumor volumes (mm3) of 9 minipigs. Volumes are based on CT Images 7, 14, 21, 28 days after implantation.

Minipig	day7		day14		day21		day28	
	Left	Right	Left	Right	Left	Right	Left	Right
1[a]	299	251	53	372	Regressed	Regressed	Regressed, Euthanized Day 28	Regressed, Euthanized Day 28
2	39	95	818	2186	3639	9239	Euthanized, Day 21	Euthanized, Day 21
3	194	145	563	224	4389	766	Euthanized, Day 21	Euthanized, Day 21
4	152	209	1219	2236	Euthanized, Day 14	Euthanized, Day 14	Euthanized, Day 14	Euthanized, Day 14
5	111	180	2260	2462	Euthanized, Day 14	Euthanized, Day 14	Euthanized, Day 14	Euthanized, Day 14
6	80	113	681	1020	4564	6672	Euthanized, Day 23	Euthanized, Day 23
7	81	174	463	551	623	3156	Euthanized, Day 23	Euthanized, Day 23
8	96	89	367	550	4694	4868	Euthanized, Day 24	Euthanized, Day 24
9[b]	67	181	305	568	1484	3432	3827, Euthanized Day 28	10690, Euthanized Day 28

[a] Tumor regression was observed from day 14 post-implantation. The minipig was euthanized at day 28 post-implantation.
[b] The minipig was euthanized at day 28 post-implantation just after the last CT acquisition.

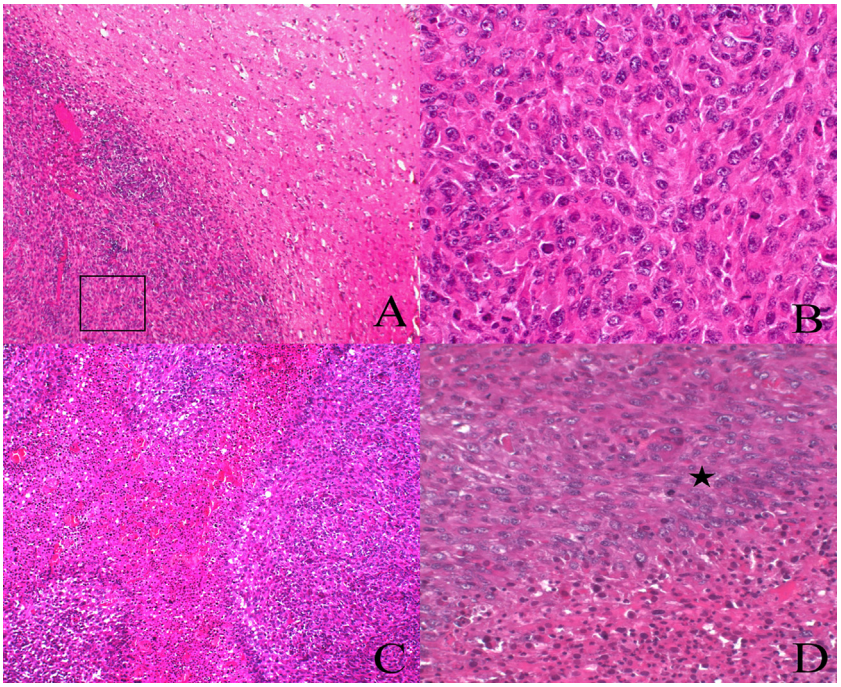

Fig. 7. Microscopic findings of U87 tumor. (A) Delimited tumor from the adjacent parenchyma, (B) enlargement of the tumor which is hypercellular and composed of polygonal to spindle cells, (C and D) tumoral cells (*) are disposed in a palisaded arrangement around necrotic foci.

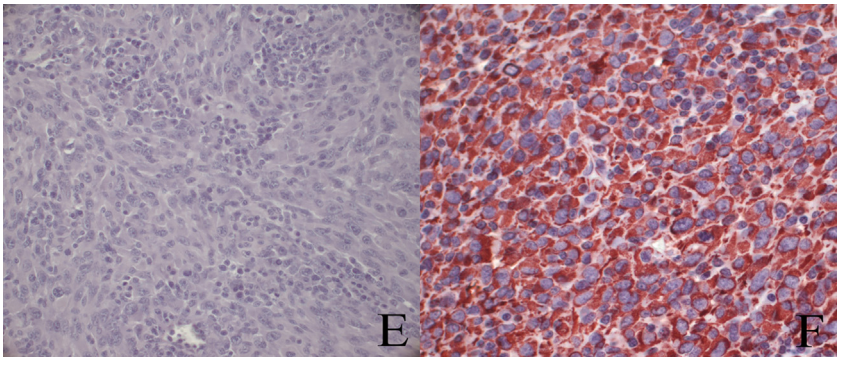

Fig. 8. Microscopic findings of U87 tumor. (E) Negative GFAP immunostaining of tumor cells (×40) and (F) showing strongly positive labeling for vimentin (×40).

Schold et al., 1987). Several attempts have been made to establish a replicable model of the human brain tumor in large animals. Most of these trials were not successful or showed the histological dissimilarity of implanted tumors in animal models when compared with its natural counterpart in humans. Some models have demonstrated limitations and variations in the size of the produced tumor. For example, GB was developed in immunosuppressed cats. The results indicated a vast range of tumor sizes (2–20 mm in diameter), over an extended period of 27–44 days after implantation (Krushelnycky et al., 1991), which is considered as a negative point for therapeutic studies. Moreover, the size and vascularization of cats' brains are very different from that of the human's brain. There-

fore, the preclinical studies in cat models with induced brain tumors take us away from the real condition of humans. Another large animal model is the spontaneous canine glioma model. The infiltrative nature of canine GB makes it an emerging and appropriate model to evaluate novel therapeutic modalities for GB (Chen et al., 2013). But there are some issues: firstly, the incidence rate of spontaneous canine GB is low and accounts for only 5% of all canine astrocytomas (Lipsitz et al., 2003; Selek et al., 2014) and providing enough large series over the short study period is quite impossible. Secondly, spontaneous tumors are heterogeneous in terms of size and location. In summary, a suitable animal model for GB should have a brain anatomy similar to humans but with a body size as small as possible which can facilitate animal handling during the studies. The tumor model should be reproducible with a predictable growth rate and the period of tumor induction should be short (Crafts and Wilson, 1977). More recently a large animal GB model was developed in a large breed pig (white Landrace) to attempt to resolve some of the previously described drawbacks of existing animal models (Selek et al., 2014). This model can be used in standardized therapeutic studies and is relevant for preclinical trials as its characteristics are similar to those of human GB (Sauleau et al., 2009; Schook et al., 2015). The main constraints remain the cost of cyclosporine adapted to the high pig weight, the housing of animals over a long period and lack of adaptation of some devices, such as the stereotactic frame. To solve these issues in this study, we selected a small breed of pig, the Yucatan minipig. All the animals were immunosuppressed by Cyclosporine. This product is widely employed in xenograft implantations in order to reduce the index of rejection (Calne, 2004; Cunha et al., 2011) through an immunosuppression with inhibition of T-cell activation. The administration of cyclosporine (Neoral®) allowed a rapid tumor growth in the brain of Yucatan minipigs. No signs of rejection were observed in all but one minipig. In this animal, the tumor regression was observed 14 days after the implantation via CT images. A reduction of cyclosporine intake (*per os*) due to the transient dysorexia in this minipig, could explain a drop of whole-blood cyclosporine concentration. The blood level was lower than 1000 μg/L in several blood samples taken after day 14 post-implantation. These results, coupled with the absence of tumors in brain histological analysis, confirmed the crucial role of an appropriate blood concentration of cyclosporine (≥1000 μg/L) on the development and maintenance of induced tumors with human xenografts in Yucatan minipigs. Following histology, 8 animals presented macroscopic tumors with radiological and anatomopathological characteristics of undifferentiated gliomas. They were not capsulated but a clear demarcation with the normal parenchyma was present and no highly infiltrative features were observed, as is the case with the U87 rodent model (Jacobs et al., 2011). Histologically, cells were polygonal to spindle in shape, highly undifferentiated with a high mitotic count. The tumors presented small to moderate areas of hypoxic necrosis, lined by cells in palisade. As in the rodent model, no glomeruloid vascular proliferation was observed (Candolfi et al., 2007). Blood vessels were present, but they were neither hyperplastic, nor were there as many as reported by Candolfi et al. in GB rodent model, and no hemorrhages were detected. Tumoral cells were positive for vimentin but negative for GFAP and S-100, as with U87 rodent models (Candolfi et al., 2007; Jacobs et al., 2011). Tumor growth rate in this Yucatan minipig model was similar to mice (Strojnik et al., 2010, 2006) and large breed pigs (Selek et al., 2014) after implantation of the U87 human cell line.

The follow-up period for Yucatan model was about 28 days. This short development time is interesting to reduce the risks of infection due to the immunosuppression induced by cyclosporine administration. Furthermore, regarding the lower weight and growth rate of Yucatan minipigs compared to a large breed pig, this proposed model is very affordable in terms of treatment, care costs and required housing space. Cyclosporine cost would be considerably lower than for large breed pigs due to the dose calculation based on the body weight (mg/kg/day). Actually, the immature large breed pigs grow rapidly, reaching 250 kg in mature adults, compared to 65 kg in 3-year-old Yucatan minipigs. Given its small size, another important advantage of the Yucatan model is its compatibility with the imaging platform used in humans and with the current stereotactic frames that can be found on the market. In summary, the reproducibility, availability and brain similarity between Yucatan minipigs and humans, make it a valuable in-vivo system for preclinical studies. Due to the size of the minipig's brain, this model is suitable for the development of new therapeutic devices that can be directly translated onto the human scale. This would allow for a more precise evaluation of different intratumoral therapy modalities, working towards the eventual goal of finding an effective treatment for this currently incurable disease. This animal model could be considered as an ideal alternative to non-human primates, which despite being an optimal choice in preclinical studies are strictly limited to use by a European directive (2008/0211).

Conflict of interest

None of the authors has any conflict of interest to disclose.

Acknowledgments

This work was supported by the Bpifrance [ISI 2013–2018]. We would also like to thank Mr. Richard Brown for assistance in the preparation and editing of this manuscript.

References

Acabchuk, R.L., Sun, Y., Wolferz, R., Eastman, M.B., Lennington, J.B., Shook, B.A., Wu, Q., Conover, J.C., Conover, J.C., 2015. 3D modeling of the lateral ventricles and histological characterization of periventricular tissue in humans and mouse. J. Vis. Exp., e52328, http://dx.doi.org/10.3791/52328.

Allahdini, F.-, Amirjamshidi, A., Reza-Zarei, M., Abdollahi, M., 2010. Evaluating the prognostic factors effective on the outcome of patients with glioblastoma multiformis: does maximal resection of the tumor lengthen the median survival? World Neurosurg. 73, 128–134, http://dx.doi.org/10.1016/j.wneu.2009.06.001.

Ashby, L.S., Smith, K.A., Stea, B., 2016. Gliadel wafer implantation combined with standard radiotherapy and concurrent followed by adjuvant temozolomide for treatment of newly diagnosed high-grade glioma: a systematic literature review. World J. Surg. Oncol. 14, 225, http://dx.doi.org/10.1186/s12957-016-0975-5.

Barani, I.J., Larson, D.A., 2015. Radiation Therapy of Glioblastoma, in: Cancer Treatment and Research. pp. 49–73. D.O.I: 10.1007/978-3-319-12048-5_4.

Buonerba, C., Di Lorenzo, G., Marinelli, A., Federico, P., Palmieri, G., Imbimbo, M., Conti, P., Peluso, G., De Placido, S., Sampson, J.H., 2011. A comprehensive outlook on intracerebral therapy of malignant gliomas. Crit. Rev. Oncol. Hematol. 80, 54–68, http://dx.doi.org/10.1016/j.critrevonc.2010.09.001.

Burger, P.C., Vogel, F.S., Green, S.B., Strike, T.A., 1985. Glioblastoma multiforme and anaplastic astrocytoma: pathologic criteria and prognostic implications. Cancer 56, 1106–1111.

Calne, R., 2004. Cyclosporine as a milestone in immunosuppression. Transplant. Proc. 36, S13–S15, http://dx.doi.org/10.1016/j.transproceed.2004.01.042.

Candolfi, M., Curtin, J.F., Nichols, W.S., Muhammad, A.G., King, G.D., Pluhar, G.E., McNiel, E.A., Ohlfest, J.R., Freese, A.B., Moore, P.F., Lerner, J., Lowenstein, P.R., Castro, M.G., 2007. Intracranial glioblastoma models in preclinical neuro-oncology: neuropathological characterization and tumor progression. J. Neurooncol. 85, 133–148, http://dx.doi.org/10.1007/s11060-007-9400-9.

Chen, L., Zhang, Y., Yang, J., Hagan, J.P., Li, M., 2013. Vertebrate animal models of glioma: understanding the mechanisms and developing new therapies. Biochim. Biophys. Acta – Rev. Cancer 1836, 158–165, http://dx.doi.org/10.1016/j.bbcan.2013.04.003.

Cokgor, I., Akabani, G., Kuan, C.T., Friedman, H.S., Friedman, A.H., Coleman, R.E., McLendon, R.E., Bigner, S.H., Zhao, X.G., Garcia-Turner, A.M., Pegram, C.N., Wikstrand, C.J., Shafman, T.D., Herndon, J.E., Provenzale, J.M., Zalutsky, M.R., Bigner, D.D., 2000. Phase I trial results of iodine-131-labeled antitenascin monoclonal antibody 81C6 treatment of patients with newly diagnosed malignant gliomas. J. Clin. Oncol. 18, 3862–3872, http://dx.doi.org/10.1200/jco.2000.18.22.3862.

Crafts, D., Wilson, C.B., 1977. Animal models of brain tumors. Natl. Cancer Inst. Monogr. 46, 11–17.

Cunha, A.M., Nascimento, F.S., Amaral, J.C.O.F., Konig, S., Takiya, C.M., Neto V, M., Rocha, E., Souza, J.P.B.M., 2011. A murine model of xenotransplantation of human glioblastoma with immunosuppression by orogastric cyclosporin. Arq. Neuropsiquiatr. 69, 112–117.
Dickinson, P.J., LeCouteur, R.A., Higgins, R.J., Bringas, J.R., Larson, R.F., Yamashita, Y., Krauze, M.T., Forsayeth, J., Noble, C.O., Drummond, D.C., Kirpotin, D.B., Park, J.W., Berger, M.S., Bankiewicz, K.S., 2010. Canine spontaneous glioma: a translational model system for convection-enhanced delivery. Neuro-Oncol. 12, 928–940, http://dx.doi.org/10.1093/neuonc/noq046.
Dinapoli, R.P., Brown, L.D., Arusell, R.M., Earle, J.D., O'Fallon, J.R., Buckner, J.C., Scheithauer, B.W., Krook, J.E., Tschetter, L.K., Maier, J.A., 1993. Phase III comparative evaluation of PCNU and carmustine combined with radiation therapy for high-grade glioma. J. Clin. Oncol. 11, 1316–1321, http://dx.doi.org/10.1200/jco.1993.11.7.1316.
Dréan, A., Goldwirt, L., Verreault, M., Canney, M., Schmitt, C., Guehennec, J., Delattre, J.-Y., Carpentier, A., Idbaih, A., 2016. Blood-brain barrier, cytotoxic chemotherapies and glioblastoma. Expert Rev. Neurother. 16, 1285–1300, http://dx.doi.org/10.1080/14737175.2016.1202761.
Ferreira, W.A.S., Pinheiro, D. do R., Costa Junior, C. da A., Rodrigues-Antunes, S., Araújo, M.D., Leão Barros, M.B., Teixeira, A.C. de S., Faro, T.A.S., Burbano, R.R., Oliveira, E.H.C. de, Harada, M.L., Borges, B. do N., 2016. An update on the epigenetics of glioblastomas. Epigenomics 8, 1289–1305, http://dx.doi.org/10.2217/epi-2016-0040.
Greene, H.S.N., 1952. The significance of the heterologous transplantability of human cancer. Cancer 5, 24–44.
Hingorani, M., Colley, W.P., Dixit, S., Beavis, A.M., 2012. Hypofractionated radiotherapy for glioblastoma: strategy for poor-risk patients or hope for the future? Br. J. Radiol. 85, e770–e781, http://dx.doi.org/10.1259/bjr/83827377.
Howells, D.W., Porritt, M.J., Rewell, S.S.J., O'Collins, V., Sena, E.S., van der Worp, H.B., Traystman, R.J., Macleod, M.R., 2010. Different strokes for different folks: the rich diversity of animal models of focal cerebral ischemia. J. Cereb. Blood Flow Metab. 30, 1412–1431, http://dx.doi.org/10.1038/jcbfm.2010.66.
Huszthy, P.C., Daphu, I., Niclou, S.P., Stieber, D., Nigro, J.M., Sakariassen, P.Ø., Miletic, H., Thorsen, F., Bjerkvig, R., 2012. In vivo models of primary brain tumors: pitfalls and perspectives. Neuro. Oncol. 14, 979–993, http://dx.doi.org/10.1093/neuonc/nos135.
Jacobs, V.L., Valdes, P.A., Hickey, W.F., De Leo, J.A., 2011. Current review of in vivo GBM rodent models: emphasis on the CNS-1 tumour model. ASN Neuro 3, e00063, http://dx.doi.org/10.1042/AN20110014.
Johnson, D.R., O'Neill, B.P., 2012. Glioblastoma survival in the United States before and during the temozolomide era. J. Neurooncol. 107, 359–364, http://dx.doi.org/10.1007/s11060-011-0749-4.
Kikuchi, T., Akasaki, Y., Abe, T., Ohno, T., 2002. Intratumoral injection of dendritic and irradiated glioma cells induces anti-tumor effects in a mouse brain tumor model. Cancer Immunol. Immunother. 51, 424–430, http://dx.doi.org/10.1007/s00262-002-0297-z.
Krementz, E.T., Greene, H.S.N., 1953. Heterologous transplantation of human neural tumors. Cancer 6, 100–110.
Krushelnycky, B.W., Farr-Jones, M.A., Mielke, B., McKean, J.D., Weir, B.K., Petruk, K.C., 1991. Development of a large-animal human brain tumor xenograft model in immunosuppressed cats. Cancer Res. 51, 2430–2437.
Lidar, Z., Mardor, Y., Jonas, T., Pfeffer, R., Faibel, M., Nass, D., Hadani, M., Ram, Z., 2004. Convection-enhanced delivery of paclitaxel for the treatment of recurrent malignant glioma: a Phase I/II clinical study. J. Neurosurg. 100, 472–479, http://dx.doi.org/10.3171/jns.2004.100.3.0472.
Lind, N.M., Moustgaard, A., Jelsing, J., Vajta, G., Cumming, P., Hansen, A.K., 2007. The use of pigs in neuroscience: modeling brain disorders. Neurosci. Biobehav. Rev. 31, 728–751, http://dx.doi.org/10.1016/j.neubiorev.2007.02.003.
Lipsitz, D., Higgins, R.J., Kortz, G.D., Dickinson, P.J., Bollen, A.W., Naydan, D.K., LeCouteur, R.A., 2003. Glioblastoma multiforme: clinical findings magnetic resonance imaging, and pathology in five dogs. Vet. Pathol. 40, 659–669, http://dx.doi.org/10.1354/vp.40-6-659.
Louis, D.N., Perry, A., Reifenberger, G., von Deimling, A., Figarella-Branger, D., Cavenee, W.K., Ohgaki, H., Wiestler, O.D., Kleihues, P., Ellison, D.W., 2016. The 2016 world health organization classification of tumors of the central nervous system: a summary. Acta Neuropathol. 131, 803–820, http://dx.doi.org/10.1007/s00401-016-1545-1.
McNeill, R.S., Vitucci, M., Wu, J., Miller, C.R., 2015. Contemporary murine models in preclinical astrocytoma drug development. Neuro. Oncol. 17, 12–28, http://dx.doi.org/10.1093/neuonc/nou288.
Michel-Monigadon, D., Nerrière-Daguin, V., Lévèque, X., Plat, M., Venturi, E., Brachet, P., Naveilhan, P., Neveu, I., 2010. Minocycline promotes long-term survival of neuronal transplant in the brain by inhibiting late microglial activation and T-cell recruitment. Transplantation 89, 816–823, http://dx.doi.org/10.1097/TP.0b013e3181cbe041.
Mujokoro, B., Adabi, M., Sadroddiny, E., Adabi, M., Khosravani, M., 2016. Nano-structures mediated co-delivery of therapeutic agents for glioblastoma treatment: a review. Mater. Sci. Eng. C 69, 1092–1102, http://dx.doi.org/10.1016/j.msec.2016.07.080.
Oh, T., Fakurnejad, S., Sayegh, E.T., Clark, A.J., Ivan, M.E., Sun, M.Z., Safaee, M., Bloch, O., James, C.D., Parsa, A.T., 2014. Immunocompetent murine models for the study of glioblastoma immunotherapy. J. Transl. Med. 12, 107, http://dx.doi.org/10.1186/1479-5876-12-107.
Omuro, A., DeAngelis, L.M., 2013. Glioblastoma and other malignant gliomas. JAMA 310, 1842, http://dx.doi.org/10.1001/jama.2013.280319.
Ostrom, Q.T., Gittleman, H., de Blank, P.M., Finlay, J.L., Gurney, J.G., McKean-Cowdin, R., Stearns, D.S., Wolff, J.E., Liu, M., Wolinsky, Y., Kruchko, C., Barnholtz-Sloan, J.S., 2016. American brain tumor association adolescent and young adult primary brain and central nervous system tumors diagnosed in the United States in 2008–2012. Neuro-Oncol. 18, i1–i50, http://dx.doi.org/10.1093/neuonc/nov297.
Pontén, J., 1975. Neoplastic human glia cells in culture. In: Human Tumor Cells in Vitro. Springer US, Boston, MA, pp. 175–206, http://dx.doi.org/10.1007/978-1-4757-1647-4_7.
Sampson, J.H., Raghavan, R., Brady, M.L., Provenzale, J.M., Herndon, J.E., Croteau, D., Friedman, A.H., Reardon, D.A., Coleman, R.E., Wong, T., Bigner, D.D., Pastan, I., Rodríguez-Ponce, M.I., Tanner, P., Puri, R., Pedain, C., Pedain, C., 2007. Clinical utility of a patient-specific algorithm for simulating intracerebral drug infusions. Neuro-Oncol. 9, 343–353, http://dx.doi.org/10.1215/15228517-2007-007.
Sauleau, P., Lapouble, E., Val-Laillet, D., Malbert, C.-H., 2009. The pig model in brain imaging and neurosurgery. Animal 3, 1138–1151, http://dx.doi.org/10.1017/S1751731109004649.
Schold, S.C., Friedman, H.S., Bigner, D.D., 1987. Therapeutic profile of the human glioma line D-54 MG in athymic mice. Cancer Treat. Rep. 71, 849–850.
Schook, L.B., Collares, T.V., Hu, W., Liang, Y., Rodrigues, F.M., Rund, L.A., Schachtschneider, K.M., Seixas, F.K., Singh, K., Wells, K.D., Walters, E.M., Prather, R.S., Counter, C.M., 2015. A genetic porcine model of cancer. PLoS One 10, e0128864, http://dx.doi.org/10.1371/journal.pone.0128864.
Selek, L., Seigneuret, E., Nugue, G., Wion, D., Nissou, M.F., Salon, C., Seurin, M.J., Carozzo, C., Ponce, F., Roger, T., Berger, F., 2014. Imaging and histological characterization of a human brain xenograft in pig: the first induced glioma model in a large animal. J. Neurosci. Methods 221, 159–165, http://dx.doi.org/10.1016/j.jneumeth.2013.10.002.
Semple, B.D., Blomgren, K., Gimlin, K., Ferriero, D.M., Noble-Haeusslein, L.J., 2013. Brain development in rodents and humans: identifying benchmarks of maturation and vulnerability to injury across species. Prog. Neurobiol. 106–107, 1–16, http://dx.doi.org/10.1016/j.pneurobio.2013.04.001.
Shaifer, C.A., Huang, J., Lin, P.C., 2010. Glioblastoma cells incorporate into tumor vasculature and contribute to vascular radioresistance. Int. J. Cancer 127, 2063–2075, http://dx.doi.org/10.1002/ijc.25249.
Snyder, J.M., Shofer, F.S., Winkle, T.J., Massicotte, C., 2006. Canine intracranial primary neoplasia: 173 cases (1986–2003). J. Vet. Intern. Med. 20, 669–675, http://dx.doi.org/10.1111/j.1939-1676.2006.tb02913.x.
Strojnik, T., Kavalar, R., Lah, T.T., 2006. Experimental model and immunohistochemical analyses of U87 human glioblastoma cell xenografts in immunosuppressed rat brains. Anticancer Res. 26, 2887–2900.
Strojnik, T., Kavalar, R., Barone, T.A., Plunkett, R.J., 2010. Experimental model and immunohistochemical comparison of U87 human glioblastoma cell xenografts on the chicken chorioallantoic membrane and in rat brains. Anticancer Res. 30, 4851–4860.
Stupp, R., Mason, W., van den Bent, M.J., Weller, M., Fisher, B.M., Taphoorn, M.J.B., Belanger, K., Brandes, A.A., Marosi, C., Bogdahn, U., Curschmann, J., Janzer, R.C., Ludwin, S.K., Gorlia, T., Allgeier, A., Lacombe, D., Cairncross, G., Eisenhauer, E., Mirimanoff, R.O., 2005. Radiotherapy plus concomitant\nand adjuvant temozolomide for glioblastoma. N. Engl. J. Med. 352, 987–996, http://dx.doi.org/10.1056/NEJMoa043330.
Tate, M.C., Aghi, M.K., 2009. Biology of angiogenesis and invasion in glioma. Neurotherapeutics 6, 447–457, http://dx.doi.org/10.1016/j.nurt.2009.04.001.
Thakkar, J.P., Dolecek, T.A., Horbinski, C., Ostrom, Q.T., Lightner, D.D., Barnholtz-Sloan, J.S., Villano, J.L., 2014. Epidemiologic and molecular prognostic review of glioblastoma. Cancer Epidemiol. Biomark. Prev. 23, 1985–1996, http://dx.doi.org/10.1158/1055-9965.EPI-14-0275.
Thomas, A.A., Ernstoff, M.S., Fadul, C.E., 2012. Immunotherapy for the treatment of glioblastoma. Cancer J. 18, 59–68, http://dx.doi.org/10.1097/PPO.0b013e3182431a73.
Walid, M.S., 2008. Prognostic factors for long-term survival after glioblastoma. Perm. J. 12, 45–48.
Weiss, T., Weller, M., Roth, P., 2016. Immunological effects of chemotherapy and radiotherapy against brain tumors. Expert Rev. Anticancer Ther. 16, 1087–1094, http://dx.doi.org/10.1080/14737140.2016.1229600.
White, E., Woolley, M., Bienemann, A., Johnson, D.E., Wyatt, M., Murray, G., Taylor, H., Gill, S.S., 2011. A robust MRI-compatible system to facilitate highly accurate stereotactic administration of therapeutic agents to targets within the brain of a large animal model. J. Neurosci. Methods 195, 78–87, http://dx.doi.org/10.1016/j.jneumeth.2010.10.023.
Yang, P., Zhang, C., Cai, J., You, G., Wang, Y., Qiu, X., Li, S., Wu, C., Yao, K., Li, W., Peng, X., Zhang, W., Jiang, T., Yang, P., Zhang, C., Cai, J., You, G., Wang, Y., Qiu, X., Li, S., Wu, C., Yao, K., Li, W., Peng, X., Zhang, W., Jiang, T., 2015. Radiation combined with temozolomide contraindicated for young adults diagnosed with anaplastic glioma. Oncotarget 7, 80091–80100, http://dx.doi.org/10.18632/oncotarget.11756.
Zagzag, D., Zhong, H., Scalzitti, J.M., Laughner, E., Simons, J.W., Semenza, G.L., 2000. Expression of hypoxia-inducible factor 1alpha in brain tumors: association with angiogenesis, invasion, and progression. Cancer 88, 2606–2618.